Light-scattering study of the mercury liquid-vapor interface

V. Kolevzon and G. Gerbeth
Forschungszentrum Rossendorf, P.O. Box 510119, 01314 Dresden, Germany

G. Pozdniakov
Institute of Theoretical and Applied Mechanics, 630090 Novosibirsk, Russia

(Received 12 August 1996)

High frequency capillary waves at a surface of mercury have been studied by means of quasielastic light-scattering spectroscopy. The observed damping constants of waves differ greatly from those predicted by the classical theoretical treatment of a Hg surface as that of a simple liquid. This effect is explained in terms of the presence of a surface layer of highly correlated atoms accompanying the Hg liquid-vapor transition. Viscoelastic properties of this layer are extracted from the fit of experimental spectra with a theoretical form utilizing a well known phenomenological model. The main conclusion of the present analysis is that the widely used hydrodynamic limit should be replaced by another form incorporating the Maxwell viscoelastic model. [S1063-651X(97)08603-0]

PACS number(s): 61.25.Mv, 68.10.Cr, 68.10.Et

I. INTRODUCTION

A liquid-metal surface has recently become a subject of different experimental and theoretical studies. Two recent experimental studies using x-ray reflectivity clearly demonstrate surface layering in mercury and liquid gallium [1,2]. Earlier theoretical predictions based on statistical pseudopotential models of an oscillatory density profile of liquid metal-vapor interface [3,4] have been confirmed in these experiments. All the above-mentioned papers postulated the existence of a highly correlated liquid metal-vapor zone with a characteristic size of a few atomic diameters into the bulk.

On the other hand, much information can be gathered from monitoring the thermally excited capillary waves intrinsic to the liquid-vapor interface. Quasielastic light scattering from capillary waves has nowadays become an important and extremely sensitive instrument to probe a liquid surface [5,6]. Only a few papers are available dealing with the application of this technique to a liquid metal surface. One of them [7] was probably the first demonstration of the structuring of the Hg surface. The experimentally observed damping constants of the capillary waves have been found above the theoretical predictions treating the surface of mercury as that of a simple liquid. The bulk viscosity inferred from these data was 3–4 times larger than its tabulated value. Such deviations could not be explained by possible errors in the data evaluation due to some improper form of the objective function. On the contrary, the instrumental width was exactly extracted from the fit of observed autocorrelation functions with an appropriate model form. Unfortunately, the paper [7] provided no evidence of how clean the sample surface was. Therefore it remains unclear up to now whether the reported effect was really a physical fact or due to the surface contamination. If the first is admitted, then it is possible to consider the surface of mercury as consisting of a structured layer, probably possessing viscoelastic properties. An attempt to extract these properties from the fit of $\Gamma(q)$ data with an appropriate model was undertaken in [8].

Theoretically neither metallic nor vaporized atoms [3] comprises this layer, which only partially covers the liquid surface. Monolayer viscoelasticity affects the propagation of the capillary waves, although up to now there has been no strong theoretical basis for the description of the surface viscoelastic properties. In a general case a liquid-vapor interface may possess up to five independent surface moduli [9,10], each involving viscous and elastic parts. In practice, however, only two of these affect the light scattering: either shear normal to the surface plane or dilational in the surface plane. These moduli comprise two elastic parts, namely, surface tension and elastic modulus, and two surface viscosities governing shear and dilation.

Two surface viscosities appear as a result of the transition from the liquid bulk (possessing isotropic properties) to the surface being strongly anisotropic. Theoretically these viscosities appear after integration the hydrodynamic equations through the interface. One might expect that surface viscosities introduced should thus scale as the difference between bulk viscosities of two adjacent phases times the thickness of the interface. It will be demonstrated how the experimentally obtained values of the surface viscosities correlate with this idea. Two theoretical studies, introducing the surface viscoelasticity differ in their theoretical formalism: in [9] these properties have been introduced for an isothermal case, while nonisothermal surface perturbations from the surface equilibrium have been incorporated into the model in [10].

Two complex surface moduli are responsible for two types of surface waves: transverse and longitudinal. These waves are intrinsically coupled, and under some circumstances even mixed [11]. Two surface viscosities play deciding roles in the mode-mixing scenario (see [6,11], and references there). In the so-called hydrodynamic limit these viscosities are introduced as dissipative parts of the surface moduli, viewed as linear response functions [12]. Such a treatment may fail in the high frequency limit pertinent to the propagation of capillary waves, as will be discussed below.

This work provides further arguments in favor of a struc-

turing of the mercury surface carefully purified, and studied over a q range extended more than hitherto. The viscoelastic properties of the mercury surface were inferred for the first time, to our knowledge, from a direct data analysis applied previously to a liquid gallium surface [13,14].

II. THEORETICAL BACKGROUND

A brief theoretical description will be given here as a basis of the further discussion. A liquid surface is subjected to continuous disturbances on the molecular level. These disturbances appear in the form of capillary waves, which in turn are due to random pressure fluctuations in the liquid bulk. The surface tension plays a role of a restoring force for short-length capillary waves which are damped by the bulk viscosity.

The linearized Navier-Stokes equation gives the dispersion equation for the propagation of capillary waves at a clean liquid surface,

$$(i\omega+2\eta q^2/\rho)^2+\gamma_0 q^3/\rho=4(\eta/\rho)^2 q^4\sqrt{1+i\omega\rho/(q^2\eta)}, \tag{1}$$

which connects the complex frequency $(\omega=\omega_0+i\Gamma)$ with the wave number q [15]. γ_0 is the surface tension and η is the bulk viscosity.

To the first order approximation the roots of the dispersion equation are given by the well-known relations [15]

$$\omega_0=\sqrt{\gamma_0 q^3/\rho}, \tag{2}$$

$$\Gamma=\eta q^2/\rho. \tag{3}$$

In the case of a liquid-monolayer interface possessing viscoelastic properties [12,9], the monolayer viscoelasticity may be described by two kinds of stress: shear and dilation. The surface tension γ_0 and the shear viscosity γ' (normal to the interface) are included in a shear modulus:

$$\gamma=\gamma_0+i\omega\gamma'. \tag{4}$$

A dilational modulus can be written as a combination of the surface elasticity and the dilational viscosity:

$$\epsilon=\epsilon_0+i\omega\epsilon'. \tag{5}$$

The dispersion equation of waves at a liquid-monolayer interface is usually written in the form [12,6]

$$\begin{aligned} D(\omega)=&[\epsilon q^2+i\omega\eta(m+q)][\gamma q^2+i\omega\eta(m+q)-\omega^2\rho/q] \\ &-[i\omega\eta(q-m)]^2 \\ =&0, \end{aligned} \tag{6}$$

where $m=\sqrt{q^2+i\omega\eta/\rho}$ and $\mathrm{Re}(m)>0$. Equation (6) can be considered as the dispersion equation of two coupled surface modes: capillary and dilational. The physical mechanism responsible for the mutual influence between two modes has been already specified [15]. Although only the capillary waves scatter light appreciably, the wave behavior depends strongly on the propagation of the dilational mode. This consequence means that the power spectrum of capillary waves will be affected by all viscoelastic interfacial properties.

The power spectrum of thermally excited capillary waves at the liquid-monolayer interface is usually written as [6]

$$P(\omega)=\frac{kT}{\omega}\frac{\tau_0 q}{\rho}\,\mathrm{Im}\left[\frac{i\omega\eta(q+m)+\epsilon q^2}{D(\omega)}\right], \tag{7}$$

where $D(\omega)$ is defined by Eq. (6) evaluated for real ω. This spectrum is not a Lorentzian; four viscoelastic properties affect the spectral shape (see, for example, [16,6]). Note that the outlined theoretical model has been developed for a liquid-monolayer system including two components. For a single-component fluid with a structured surface, there is no adequate theoretical description of surface viscoelasticity; we will try to adopt the existing theories below.

III. EXPERIMENTAL METHODS

A single wave of wave number q scatters light at a well-defined angle δq from the specular reflection. The wave number q is related to the scattering angle $\delta\theta$ as

$$q=\frac{2\pi}{\lambda_0}\cos\,\theta_0\,\delta\theta, \tag{8}$$

where λ_0 is the wavelength of the light source and θ_0 the angle of incidence.

Heterodyne light beating spectroscopy [18] has been used to detect the very low frequency shifts. The scattered light with electric field amplitude E_s is mixed with a reference beam of amplitude E_r (ideally time independent). The output photocurrent is given by

$$I(t)\approx|E_r|^2+|E_s|^2+2\,\mathrm{Re}[E_r^* E_s\,\exp(i(\omega_r-\omega_s)t)], \tag{9}$$

so that $I(t)$ consists of a dc component (in the ideal case) plus a heterodyne-beat term at the Doppler-shifted frequency.

The details of operation of the light-scattering spectrometers may be found elsewhere [19,13]; therefore only a brief description will be given here. A beam from a 5-mW He-Ne laser (TEM_{00}, $\lambda=632.5$ nm) fell on the liquid metal surface at an angle of approximately 20°. A diffraction grating, imaged onto the liquid surface, provided a set of reference beams (I_r), being thus spatially coherent with the scattered light (I_s). Different magnitudes of the I_r/I_s ratio were obtained by means of low density optical filters. The signal from an avalanche photodiode was fed to the spectrum analyzer (Spectroscopic Instruments). The whole apparatus was placed on an optical table (Melles Griot), vibration isolation being supplied with four air pressured cylinders mounted into the legs.

The scattering angles $\delta\theta$ were determined from photograph of the diffraction spots taken with a charge coupled device (CCD) camera at two positions along the beam.

A. Materials and sample cell design

As distinct from liquid gallium, mercury has a lower oxidation ability; therefore the requirements for preparation of a Hg surface are substantially lower. Nevertheless, if mercury is exposed to open air the surface is immediately covered by a very thin layer of oxide. This layer is so thin that it does

not scatter light appreciably, and only becomes detectable by eye after some manipulation producing mechanical stress on the oxide film.

A clean Hg surface was obtained inside a metal chamber having a diameter of 10 cm and a height of 9 cm, and supplied with a vacuum flange and an optically polished glass window. About 5 ml of liquid Hg (99.998%, Merck) was loaded in the open air into a Teflon vessel placed inside the chamber. The vessel terminating in a stainless steel tube (of a diameter 3 mm) was fixed to the chamber, so that the end of the tube was located just above the working trough. The upper end of the tube was tightly closed with a shutter machined from teflon. The chamber was sealed with an indium ring (between optical window and metal flange), and pumped down to a pressure of about 10^{-2} Torr. Then it was overpressed with a standard mixture of Ar/(5% H_2) (spectroscopic purity) and evacuated again. This cycle repeated several times allowed for degassing the mercury in the vessel. The main reason for the choice of hydrogen is that it can reduce any mercury oxide present. To ensure that no oxide comes from the vessel through the tube, its upper end was perfectly wetted by Hg prior to use. The shutter could be opened with a small relay connected to the outer power supply. The working trough of a diameter 70 mm was machined from Ti to a special form providing a depth of 2 mm in the middle. Before installing the chamber, the trough and the filling vessel were cleaned with chromic acid and carefully rinsed in double distilled water. After the valve in the vessel was opened only a part of Hg was dropped to the trough, while the rest remained in the vessel together with the oxide film.

The mercury surface in the trough was mirror reflecting without any visible traces of contamination. A laser beam specularly reflected from the liquid surface did not display any speckles, typically caused by scattering from a rough oxidized surface. The depth of the Hg layer appeared to be about 2 mm; no efforts were applied to achieve wetting behavior. Nevertheless, the surface was relatively flat, as confirmed by the minimal divergence of the reflected beam. The temperature was measured with a thermocouple (diameter 0.2 mm) glued to the trough.

Mercury analyzed after the experiment with atom-absorption spectroscopy did not display any impurities (except gold) down to the sensitivity limit of this technique. Gold found in concentration of 0.0018 (mass %) could not influence the surface properties.

B. Instrumental effect

A typical spectrum is shown in Fig. 1. The data are fitted with a theoretical function accounting for the effect of instrumental broadening: it arises from the illumination of more than one wave vector q on the liquid surface. The spread δq in the wave vectors gives a correspondent broadening in the frequency. A convolution between an ideal spectrum having the Lorentzian shape and a Gaussian instrumental function of width β (in the frequency domain) gives the form [20,21]

$$P(\omega)=\int_{-\infty}^{\infty}\frac{(\Gamma/\beta)\exp[-(\omega-\omega')^2/\beta^2]}{\Gamma^2+(\omega'-\omega_0)^2}\,d\omega'. \quad (10)$$

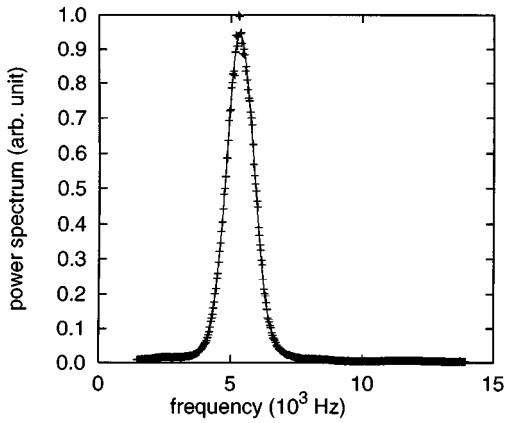

FIG. 1. A typical power spectrum of the light scattered by the free surface of mercury at $q=323\ \mathrm{cm}^{-1}$. The solid line is the fitting theoretical function in the form of Eq. (11).

This integral can be solved in terms of a complementary error function of the complex argument [21,22],

$$P(\omega)=A\,\mathrm{Re}[\exp(-[i\Gamma/\beta+(\omega-\omega_0)/\beta]^2)\times\mathrm{erfc}(-i[i\Gamma/\beta+(\omega-\omega_0)/\beta])]+B \quad (11)$$

where A is the scaling amplitude and B the background. Five properties were extracted from the fit of experimental spectra: wave frequency ω_0, damping constant Γ, instrumental width β, amplitude A, and background B. To ensure that the beam has a Gaussian profile, its shape was checked in the photodetector plane by digitizing video images of the diffraction spots and subsequent analyzing the intensity distribution across the spots.

The experimentally observed values of β can be compared with the theoretical estimations. Following the ideas summarized in [23], one can obtain a broadening Δq corresponding to the Gaussian beam of a width D (at $1/e$ positions at the beam profile) on the liquid surface,

$$\Delta q=\frac{4\sqrt{\ln 2}}{\pi D}\cos\,\theta, \quad (12)$$

where θ is an angle of incidence. The corresponding broadening in frequency β is given by $\beta=\Delta q(d\omega/dq)$. If the roots of the dispersion equation are taken in the form of Eq. (2), the instrumental width is defined by

$$\beta=\frac{6\sqrt{\ln 2}}{\pi D}\cos\,\theta\sqrt{q\gamma_0/\rho}. \quad (13)$$

For the case of liquid metals having large surface tensions and relatively small kinematic viscosities, a precise knowledge of the instrumental width is very important, since it dominates the spectral width (at least at low and moderate q) and, of course, cannot be neglected in the data analysis. It might, in principle, be possible to evaluate β from the direct measurements if the surface tension were known. In the present study it is definitely not the case. Nevertheless, the estimates of β inferred from the fit can be verified with those derived from direct measurements on the basis of Eq. (13) if the surface tension is supposed to have its accepted value. It

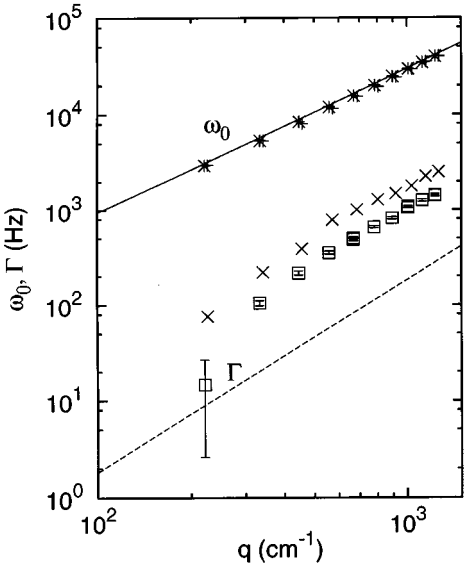

FIG. 2. Peak frequencies (∗) and damping constants (□) of capillary waves at the surface of mercury. The lines are the theoretical predictions of the dispersion behavior based upon the following values of the physical properties of mercury: γ_0=475 mN/m, η=1.55 mPa s, and ρ=13.5 g cm^{-3}. ω_0 and Γ collected from the Hg/HgO interface are shown with (+) and (×), respectively.

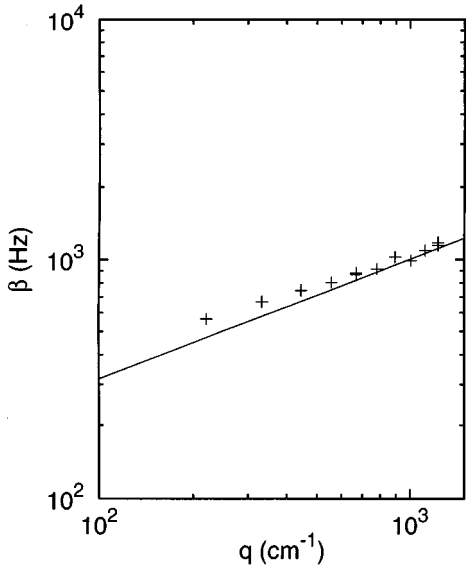

FIG. 3. The instrumental width extracted from the fit shown together with the theoretical prediction Eq. (13) for our experimental geometry with θ_0=22°, D=3.5 mm, and accepted values of γ and ρ. The errors are smaller than the plotted points.

is clearly apparent from Eqs. (2) and (13) that the ratio Γ/β is an increasing function of q. This means that β should have a smaller effect at higher wave numbers.

Vibrational disturbances were significant only for spectra collected at q=122 cm^{-1}, corresponding to the first diffraction order. These data have been omitted from our analysis.

IV. RESULTS OF CLASSICAL DATA ANALYSIS

A theoretical model treating a liquid metal surface as that of a simple fluid is referred here as a classical model. The experimental values of ω_0 and Γ are shown in Fig. 2 together with such theoretical expectations in the form of Eqs. (2) and (3), respectively. The values of the peak frequency differ only slightly from the theoretical dependence, though the $q^{3/2}$ variation is clear. However, the damping constants deviate by a factor of 3–4 from the theoretical line. The ω_0 and Γ data at high q are in good accord with those of Bird and Hills [7], although their data have been recovered in the time domain, without using a diffraction grating for heterodyning, and therefore covered a smaller q range. We note that at low q the present Γ data display a tendency toward the classical Γ line, which differs essentially from those of [7].

There remain some doubts whether the reported effect could be attributed to the presence of an oxide film. In order to demonstrate the influence of HgO on the capillary waves the liquid surface was exposed to air and light-scattering experiment was repeated. Observed ω_0 and Γ are shown in Fig. 2 as well. As can be seen, the striking difference appears in damping constants collected from the oxidized sample and those with the free surface.

Analysis of the experimental spectra by means of a fit to a convolution of a Lorentzian with a Gaussian is well established for the evaluation of Γ and ω_0 (at least in the time domain). Large anomalies in Γ do not appear as a result of an improper data analysis, but must be due to the incorrect treatment of the surface of mercury as a simple fluid. The instrumental width in the frequency domain obtained from the fit is shown in Fig. 3. The line for β is not a fit, but displays the theoretical β behavior for the present experimental geometry and a given value of the tension of 475 mN/m.

One may suggest that the highly correlated layers of ''double-state'' atoms adsorbed from the vapor at the liquid surface [3] cause the high damping. The real thickness of the surface zone is not reflected in the capillary wave dispersion equation; therefore the word ''monolayer'' will be used only conditionally. Such a monolayer can possess nonzero elasticity, as its compressibility is different from that of the bulk.

Incorporation of surface viscoelasticity into the dispersion equation leads to drastic changes of Γ for capillary waves but only minor changes in ω_0. The dilational modulus ϵ_0 has the strongest influence on Γ and ω_0 due to the intrinsic coupling between transverse and longitudinal waves on the liquid-monolayer interface (see for example [8,6]). In particular, both the peak frequency and the damping rise when the ratio ϵ_0/γ_0 increases starting from zero. The maxima for Γ and ω_0 appear near ϵ_0/γ_0=0.16, as a point of resonance between two surface modes.

V. DIRECT SPECTRAL FIT

It is strongly desirable to extract the values of viscoelastic properties from each experimentally observed spectrum using a multiparametric fit by a functional form involving four interfacial properties. The method of direct fitting has been developed in the frequency domain, taking into account the instrumental effect and using the autocorrelation function of the scattered light $F^{\mathrm{FT}}[P(\omega)]$ established in [16]

$$\hat{P}(\omega)=\frac{1}{2\pi}\int_{-\infty}^{\infty}\exp(-i\omega\tau)F^{\mathrm{FT}}[P(\omega)]\exp(-\beta^2\tau^2/4)d\tau, \tag{14}$$

omitting some constant factors. Here $P(\omega)$ is given by Eq. (7), and β is an instrumental width in the time domain. The data were fitted by a functional calculated in 400 points:

$$F=\sum_{i=1}^{400}[P(\omega_i)-A\hat{P}(\omega_i;\gamma_0,\beta,\epsilon_0,\epsilon',\gamma',\eta)+B]^2/\delta_i^2. \tag{15}$$

Since each experimentally collected spectrum was averaged over 500 scans, the fractional error δ_i at each experimental point tends to zero (in the limit of infinite number of averaging), therefore equal weightings were used. The errors on the fitted parameters were estimated as 68.3% confidence limits. The objective function $\hat{P}$ represents the theoretical spectrum depending on eight parameters: the four viscoelastic properties γ_0, ϵ_0, ϵ', and γ', instrumental width β, bulk viscosity η, amplitude factor A, and constant background B. The reason for including the bulk viscosity in the fit was purely to test the correctness of the model. If the postulated effect of high Γ is caused by the surface elasticity, then the bulk viscosity returned by the fit should not deviate too much from the well-known tabulated value.

The fitted values of the bulk viscosity lie between 1.2 and 1.4 cP, close to the tabulated $\eta=1.55$ cP. One can conclude that the fit of experimentally observed spectra confirms the existence of two contributions to the spectral width: one from the damping of capillary waves by the bulk viscosity of mercury, and another from viscoelasticity of the surface layer. The fit was of the same quality as that shown in Fig. 1. Only at high $q(q>1000\ \mathrm{cm}^{-1})$ was the noise in the data apparent at the spectral wings leading to the large residuals. The noise in the data originates in the shot noise at the photodetector.

The γ_0 and γ' data from the fit for various values or q are plotted in Fig. 4. The γ_0 points display a tendency to decrease with q, which could be attributed to Maxwellian relaxations. The results for γ' were quite surprising: the negative values were obtained at low and moderate q. A wide variety of starting points has been tested, and only those solutions satisfying the relevant statistical criteria are chosen for the final values of the fitted parameters. As was shown in [24], γ' might in principle be negative. In that case γ' was not considered as an independent property, but as reflecting the variations of the surface excess entropy (for a one-component system). The physical consequences following from the negative γ' will be specified below.

Let us turn to the dilational viscoelasticity shown in Fig. 5. Since ϵ_0 is the main parameter influencing the spectral width, the convergence of the fit was somewhat dependent on the initial values of ϵ_0. The sensitivity of the objective function to the two surface viscosities is much lower than that for ϵ_0. The surface dilational modulus can be introduced as for an insoluble monolayer:

$$\epsilon_0=-\Gamma_s\frac{d\gamma_0}{d\Gamma_s}, \tag{16}$$

where Γ_s is the surface concentration. In the present case, Γ_s refers to the surface concentration of the highly correlated atoms, partially covering the surface of the liquid metal [3]. The values of ϵ_0 oscillate in the range between 10 and 20 mN m^{-1}. Note that for almost all q our extracted values of ϵ_0 were 2–3 times lower than those at the surface mode resonance. The values of ϵ_0 extracted from the fit contradict those ($\epsilon_0=310$ mN m^{-1}) found by Earnshaw's analysis [8]. This contradiction is explained by different approach to fitting the experimental Γ at various q. In [8] the fit involved the q dependence of Γ derived from the solution of the dispersion equation (6). When all viscoelastic properties may be q dependent, such a fit cannot be appropriate.

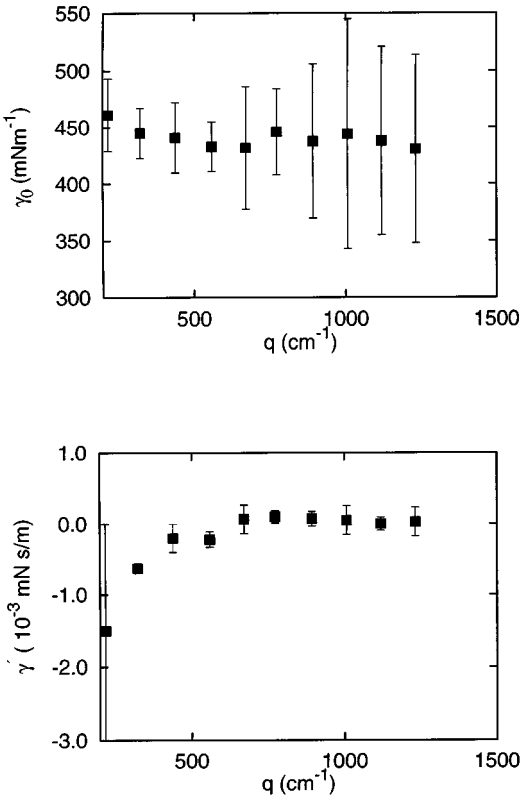

FIG. 4. The data of the surface tension γ_0 and the transverse shear viscosity γ' deduced from the direct spectral fit in the form of Eq. (15).

The central estimates of ϵ' and γ' oscillate between the negative and positive values for different q. The precision of evaluation of two surface viscosities decreases at high q due to the lower signal to noise ratio. The weighted averages of all surface properties calculated for all q are interesting enough to be presented here: $\gamma_0=446$ mN/m, $\epsilon_0=16.4$ mN/m, $\epsilon'=0.9\times10^{-5}$ mN s/m, and $\gamma'=-1.2\times10^{-4}$ mN s/m.

The value of ϵ', though nonzero, is an order of magnitude less than that of γ'. The two viscosities reflect the rate of strains in two different planes: in the plane of interface and normal to it. The absolute values of the surface viscosities point to very small relaxations (or nearly infinite speed) of compression parallel to the surface and oscillation with essentially nonzero relaxation time for normal shear stresses. The main result of this statistical analysis is the negative averaged value of γ'. This may indicate a loss of stability of capillary waves (see below), or result from the incompleteness of the theoretical model.

The values of the surface viscosities can be compared with the bulk shear viscosity if the thickness of the interfa-

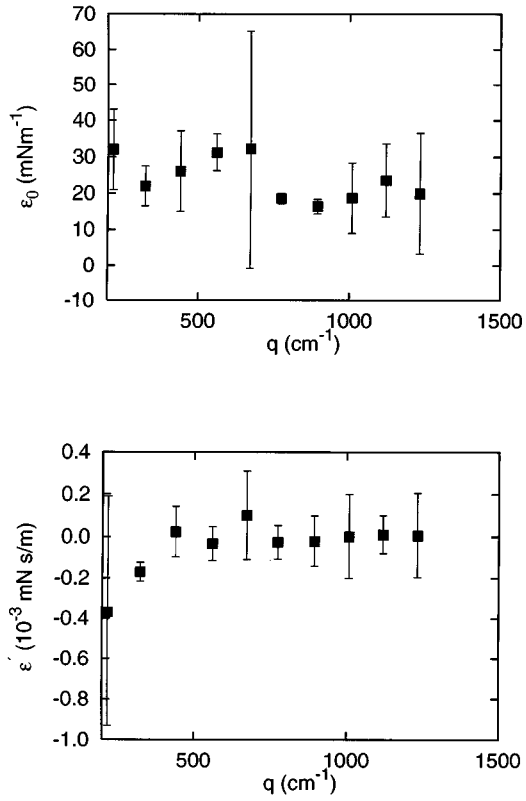

FIG. 5. The surface elastic modulus ϵ_0 and the dilational surface viscosity ϵ' extracted from the direct fit using Eq. (15).

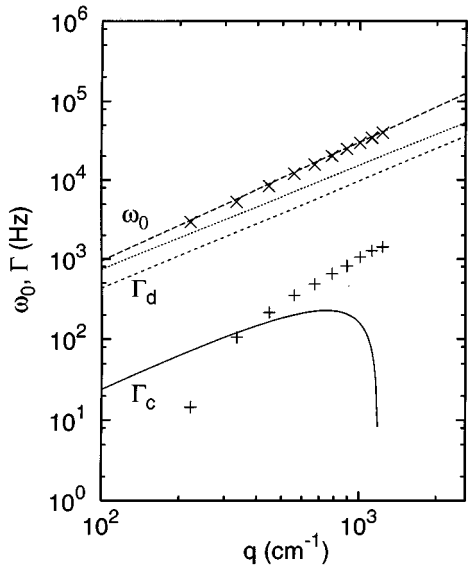

FIG. 6. Numerical solutions of the dispersion equation Eq. (6) for a Hg free surface together with the experimentally observed ω_0 ($\times$) and Γ ($+$). The viscoelastic properties are those extracted from the direct fit after the global averaging: $\gamma_0=445$ mN/m, $\gamma'=-2.8\times10^{-5}$ mN s/m, $\epsilon_0=16$ mN/m, and $\epsilon'=1\times10^{-6}$ mN s/m. Γ_c and Γ_d denote the damping of capillary and dilational waves, respectively. The damping of the capillary mode tends to negative values (not shown): the wave destabilization is clearly apparent.

cial zone is defined. If, say, it is taken as high as 10 nm, then the magnitude of the bulk viscosity, calculated as the surface viscosity divided by the interfacial thickness, will be about 10^4 times larger than is usually assumed. We believe that such huge discrepancy reflects the fact that surface viscosity (either dilational or normal shear) *cannot* be regarded as a surface excess property comprising the difference between bulk viscosities of two adjacent phases. Therefore the above-mentioned scaling behavior is incorrect. It seems reasonable to suppose that the surface viscosity should be scaled as the bulk one times the wavelength of the capillary wave. This implies that those processes responsible for the surface viscoelasticity take place in a region much thicker than the width of the interface. One rather striking example of these processes in a system of a soluble adsorbed monolayer is the competition between adsorption-desorption and diffusion in the concentrational boundary layer beneath the surface. As claimed in [17,14], the surface dilational viscosity can be fully accounted for in the frame of this model. The main result of this formalism is that ϵ' (as well as ϵ_0) are not independent properties but, in fact, depend on some relaxation time, which is a function of the diffusion coefficient and the slope of the adsorption isotherm. Unfortunately, for a one-component system (such as pure mercury) such a theoretical treatment must be inadequate.

VI. DISPERSION EQUATION

In the following discussion we concentrate upon the interpretation of the γ' data. Although negative γ' was reported earlier for the surface of alkanes [24], a direct analogy with the present case would be incorrect. The main difference is that the Γ data of [24] were found below the classical line, while those data observed in the present study lay well above. We first address the question whether the dispersion equation (6), solved using the values of the surface properties, could clarify the effect of negative γ'.

Figure 6 demonstrates the solutions of Eq. (6) for averaged values of viscoelastic properties found from the fit. The most important feature of this plot is that the damping constants of the capillary wave continuously decrease and become negative due to $\gamma'<0$ for $q>1000$ cm^{-1} (not shown). Negative Γ implies an exponential growth of wave amplitude. Although wave destabilization is well known for systems with heat or mass flux through the interface (as in the case of Marangoni convection, for instance) its direct application to thermally excited capillary waves seems to be disputable due to the absence of an energy source for the growth of disturbances in a closed system lacking steady fluxes or applied fields.

The other possibility is that the introduction of γ' in the hydrodynamic limit is incorrect. Indeed, this approach implies that the effect of the surface viscosity rises proportionally to ω [see Eq. (4)]. From a comparison with the usual hydrodynamics it is quite clear that this cannot be the case, because viscous effects are known to be important only in the limit of low and moderate frequencies, while at high ω inertia takes over. Thus one may use the Maxwell model including correct asymptotic behavior (at low and high ω) for establishing the solution of the dispersion equation. In the framework of this model the properties of a structured surface layer can be characterized by the elastic (γ_s) and the viscous (γ') parts connected via some relaxation time τ responsible for the relaxation of oscillatory shear stresses:

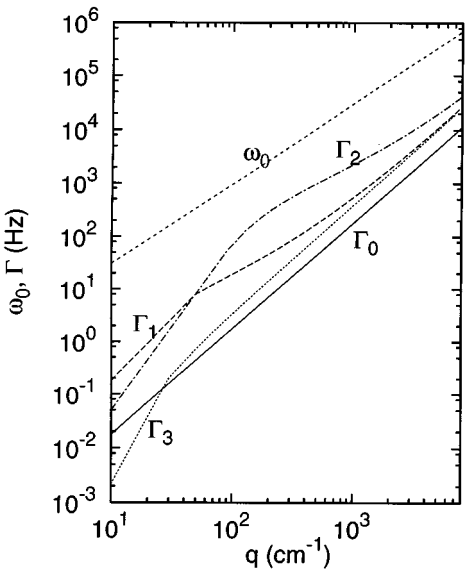

FIG. 7. Dispersion relations [Eq. (18)] for the purely transverse mode (capillary wave) on a liquid surface possessing a normal shear viscoelastic modulus γ_s and viscosity γ'. The bulk properties were chosen as for pure mercury. For all the curves, $\gamma_s=3\times10^{-5}$ mN/m. The lines denoted by Γ_0, Γ_1, Γ_2, and Γ_3 were calculated for the surface shear viscosities $\gamma'=0$, 5×10^{-5}, 4×10^{-6}, and -5×10^{-5} (mN s/m) respectively. The solutions for ω_0 coincide for all values of the surface viscosity γ'.

$\tau\sim\gamma'/\gamma_s$ [25]. Then the complex shear modulus (frequency dependent) acting normal to the surface plane is expressed via the equilibrium surface tension γ_0, an elastic modulus γ_s and the transverse shear viscosity γ':

$$\gamma(\omega)=\gamma_0+\frac{-i\omega\gamma_s\gamma'}{\gamma_s-i\omega\gamma'}. \tag{17}$$

In other words, the surface tension comprises two parts: steady and oscillatory.

We may find out the agreement between experimentally detected ω_0 and Γ and the solution of the dispersion equation for pure capillary waves propagating at the structured Hg surface. Substituting Eq. (17) into the dispersion equation (1), we find

$$(i\omega+2\eta q^2/\rho)^2+q^3\rho\left(\gamma_0+\frac{-i\omega\gamma_s\gamma'}{\gamma_s-i\omega\gamma'}\right)$$
$$=4(\eta/\rho)^2q^4\sqrt{1+i\omega\rho/(q^2\eta)} \tag{18}$$

We are not aware of solution of the dispersion equation (18), whereas it may highlight the q behavior of the capillary damping. Before the direct comparison with experiment, it is worth establishing the solutions of Eq. (18) for some values of the surface properties.

The results of numerical solution of the modified dispersion equation (18) are shown in Fig. 7 for different γ'/γ_s. The specific choice of γ_s is made to keep the ω_0 line unalterable while studying the change of Γ for different surface viscosities varied in a wide range. Such a choice is dictated by the trends in the experimental data: the points of ω_0 deviate negligible from the theoretical line described by Eq. (2), whereas there is no simple theoretical dependence for the Γ points. The plot demonstrates that the damping constants deviate significantly from the solid line [given by Eq. (3)], but the peak frequencies remain essentially the same. It is instructive to comment briefly on the behavior of the plotted lines. The transverse shear viscosity is assumed at first to be positive and varied in the range $10^{-6}<\gamma'<10^{-4}$ mN s/m but γ_s is fixed: $\gamma_s=3\times10^{-5}$ mN/m for all the curves. In the range $10^{-5}<\gamma'<1\times10^{-4}$ mN s/m the Γ behavior is very similar to the curve denoted by Γ_1: a maximum deviation from the q^2 law is observed for the wave numbers $q<100$ cm^{-1}, which are below the experimentally accessible q. For those q studied the slope of the Γ_1 curve does not agree with the trends in the experimental data (see Fig. 2). For $\gamma'<6\times10^{-6}$ mN s/m the Γ behavior, depicted by the Γ_2 curve, changes drastically: it deviates largely from q^2, and diverges from the solid line for $100<q<3000$ cm^{-1}, but for $q<100$ and $q>9000$ (cm^{-1}) the viscoelastic Γ converges slowly to those of an ideal surface. It is interesting to note that if both γ_s and γ' are negative, Γ remains positive up to certain values of γ_s and γ' (shown with the Γ_3 curve). In particular, Γ of capillary waves becomes negative at $q<10$ cm^{-1} for $\gamma'=-5\times10^{-5}$ mN s/m and $\gamma_s=-5\times10^{-3}$ mN/m. As mentioned above, the negative Γ of waves cannot be admitted as a physical fact, hence the magnitudes of γ_s and γ' providing negative damping should be considered as natural limitations on the surface shear viscosity and surface elastic modulus.

This Γ behavior is too complicated to be explained without estimating the magnitudes of the leading terms in the dispersion equation, which is far from the subject of the present study. Nevertheless, some simple interpretations of the Maxwell formula [Eq. (17)] involving identification of the relaxation time as $\tau\sim\gamma'/\gamma_s$ can be useful. In the limit of very low frequency ($\omega\tau\ll1$) the surface elasticity vanishes, and the damping of capillary waves is mainly due to the surface and bulk viscosities. At a high frequency asymptote ($\omega\tau\gg1$), the surface behaves like a ''solid'' possessing only the elasticity. In this case, if γ_s is small enough to influence ω_0, the frequency dependence of the surface complex modulus vanishes, and the damping behavior resembles that of a pure surface which is apparent from the curves at $q>8000$ (cm^{-1}). In the intermediate range of $\omega\sim\tau^{-1}$, the surface displays a viscoelastic response reflected in the graph $\Gamma_1(q)$.

It is instructive to see how the experimentally observed Γ can be described by the modified dispersion equation. Figure 8 shows the experimental data again, together with the best fit solution for the damping constant derived from Eq. (18). The experimental data for capillary wave Γ with that found from the modified dispersion equation (Γ_1) demonstrates relatively good agreement at high q, whereas at low q the fit is very poor. In order to see how the effect of high damping could be accounted for by the transverse shear modulus alone, the experimental spectra were refitted by the usual model but with the constrains $\epsilon_0=\epsilon'=0$. Despite the small deviations between the theoretical and experimental points the variances on γ_0, γ', and η were enormous. One can conclude that the fit with the present theoretical form fails to derive correct estimates of the surface parameters if only the transverse complex modulus is incorporated into the objective function.

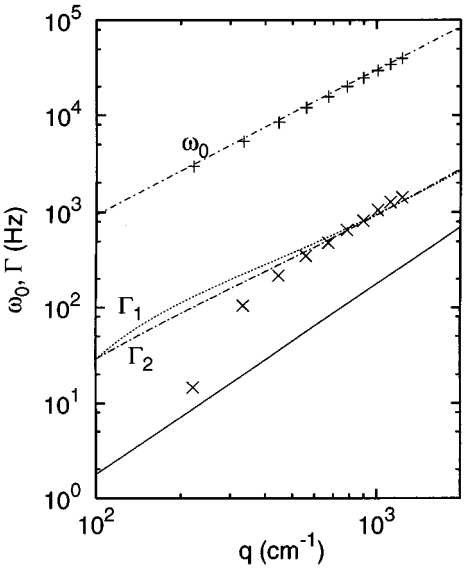

FIG. 8. Dispersion relations for purely transverse wave vs coupled longitudinal-transverse ones. Damping constants are as follows: Γ_1 is the best-fit solution with the Maxwell model only [$\gamma_0=465$ and $\gamma_s=9\times10^{-3}$ (mN/m), and $\gamma'=1\times10^{-6}$]. Γ_2 is the capillary-dilational wave damping: $\gamma_0=465$ and $\epsilon_0=23$ (mN/m), and $\gamma'=\epsilon'=0$. Classical damping for the free Hg surface is shown with the solid line. The peak frequencies ω_0 coincide in all cases. Experimentally observed ω_0 and Γ are shown with + and $\times$, respectively.

We turn to the dilational modulus to seek an explanation for the q behavior. Unfortunately the widely used phenomenological model does not explain the origin of ϵ_0: it is introduced there either as the surface excess property (arising from the difference between compressibility in the bulk and liquid surface) or as an equilibrium constant inherent in an insoluble monolayer on top of a liquid. For pure liquids without surface structure $\epsilon_0=0$, only the transverse oscillations are sustained at the surface. In the frame of the conventional model, considering soluble and insoluble films, the elasticity appears as a result of the feedback reaction of the film on compression. In the case of a highly correlated layer on top of liquid metals, such a reaction is not obvious: the ''correlated'' (or ''double state'') atoms being compressed by the longitudinal wave could easily diffuse to the bulk, and the surface elasticity might not appear. On the other hand, the equilibrium concentration of the correlated atoms should be constant at a fixed temperature. This implies that temperature disturbances arising from compression of surface atoms could be responsible for restoring the initial value of Γ_s. In this case the surface elasticity appears as a result of quick (nearly adiabatic) compression in the surface plane instead of slow isothermal compression introduced for the classical case of films on a liquid surface. ϵ_0 has been treated in [10] as an analog of the volume compressibility responsible for propagation of longitudinal sound waves. Such an approach cannot be considered here due to the huge difference between the phase velocity of capillary waves (typically a few m/s) and the speed of sound in mercury (1500 m/s). ϵ_0 is considered here only as a ''phenomenological'' property due to the lack of a precise theoretical definition of surface elasticity in the case of a one-component liquid with structured surface.

A solution of the dispersion equation for $\epsilon_0\neq0$ is shown in Fig. 8 with the line depicted as Γ_2. The value of the transverse shear viscosity was assumed equal to zero in order to demonstrate the pure effect of the dilational modulus. In this case the dispersion solutions display strong coupling between transverse and longitudinal modes. The mode mixing predicted in [11] manifests itself in convergence of the Γ of capillary waves and Γ of dilational ones for $q>1000$ cm^{-1}. For the range of q presently studied, the damping of capillary waves does not display such a tendency (at least if the phenomenological model is used for interpretation of surface wave behavior). The best theoretical line describing experimental Γ points is that of $\epsilon'=0$ and $\gamma'=0$. This line is also shown in the plot. In this case the agreement with the experimental data (especially at low q) is rather poor. The main essence of the outlined analysis is that neither dilational elasticity nor transverse shear alone can fully describe the dispersion behavior of capillary waves on mercury in the experimentally studied q range.

VII. CONCLUSIONS

This work demonstrates that light scattering from thermally excited capillary waves can be successfully used to investigate the surface properties of molten metals. If the instrumental broadening is included in the data analysis, the evaluation of light-scattering data gives unbiased estimates for ω_0 and Γ of the surface capillary waves.

In the first stage of analysis, the value of surface tension derived from the observed peak frequencies at ten angles is found to be in good accord with classical data. Large anomalies have been detected for the damping coefficient of the capillary waves with respect to the assumption of a simple liquid influencing the wave damping only via the bulk viscosity. Since strong precautions were taken against the oxidation of Hg surface, the reported anomalies could not be caused by the surface oxide. Hence it is assumed that a highly correlated surface layer possessing viscoelasticity affects the surface waves.

Four viscoelastic properties of the Hg surface were, for the first time to our knowledge, extracted from the direct spectral analysis. The weighted average of the normal shear viscosity over the whole experimentally accessible q was negative. This would lead to a destabilization of capillary waves, as can be recognized from numerical solutions of the dispersion equation. However, the wave destabilization cannot be understood in the absence of either steady fluxes or external temperature gradients. Thus the inadequacy of the theory introducing the surface viscosity in the hydrodynamic limit must be admitted.

The effect of a complex transverse shear modulus introduced through the Maxwell relaxation model and substituted into the Lamb-Levich dispersion equation has been studied numerically using values of the surface viscoelastic properties relevant to those found from a many-parametric fit. The principal effect of introducing the complex shear modulus is to increase the capillary wave damping. The experimental $\Gamma(q)$ behavior is described quite well by this complex shear modulus only at high q, whereas at low q the agreement is poor.

It should be stressed that neither $\gamma(\omega)$ nor ϵ_0 alone (as introduced in the widely used model) can completely describe the observed $\Gamma(q)$ dependence. Some processes, like the disturbances of the temperature or electric charge density at a liquid surface, were not accounted for in the framework of the existing theoretical model, but in fact might be important for the occurrence of the dilation viscoelasticity [26]. Hence an adequate theory describing viscoelasticity of a one-component liquid surface would be strongly desirable for the successive application of light-scattering technique.

ACKNOWLEDGMENTS

This research was supported by a Grant from the G. I. F, the German-Israeli Foundation for Scientific Research and Development. We are particularly grateful to Professor J. C. Earnshaw of Queen's University, Belfast for stimulated discussions, comments, and a critical reading the manuscript. Fruitful discussions were shared with J. Priede, Forschungszentrum Rossendorf. One of us (G.P.) wishes to thank Forschungszentrum Rossendorf for financial support.

[1] O. M. Magnussen, B. M. Ocko, M. J. Regan, K. Penanen, P. S. Pershan, and M. Deutsch, Phys. Rev. Lett. **74**, 22 (1995); **74**, 4444 (1995).
[2] M. J. Regan, E. H. Kawamoto, S. Lee, P. S. Pershan, N. Maskil, M. Deutsch, O. M. Magnussen, B. M. Ocko, and L. E. Berman, Phys. Rev. Lett. **75**, 13 (1995); **75**, 2498 (1995).
[3] M. P. D'Evelin and S. A. Rice, J. Chem. Phys. **78**, 5225 (1982).
[4] J. G. Harris, J. Griko, and S. A. Rice, J. Chem. Phys. **87**, 3069 (1987).
[5] *Light Scattering by Liquid Surfaces and Complementary Techniques*, edited by D. Langevin (Dekker, New York, 1992).
[6] J. C. Earnshaw and E. McCoo, Langmuir **11**, 1087 (1995).
[7] M. Bird and G. Hills, in *Physicochemical Hydrodynamics*, edited by D. Spalding (Advance, London, 1977), p. 609.
[8] J. C. Earnshaw, Phys. Lett. **18**, 40 (1982).
[9] F. C. Goodrich, Proc. R. Soc. London Ser. A **374**, 341 (1981).
[10] M. Baus and C. F. Tejero, Chem. Phys. Lett. **84**, 2 (1981); **84**, 222 (1981); M. Baus and C. F. Tejero, J. Chem. Phys. **78**, 1 (1983); **78**, 483 (1983).
[11] J. C. Earnshaw and E. McCoo, Phys. Rev. Lett. **72**, 1 (1994); **72**, 84 (1994).
[12] L. Kramer, J. Chem. Phys. **55**, 5 (1971); **55**, 2097 (1971).
[13] V. Kolevzon and G. Gerbeth, J. Phys. D **29**, 2071 (1996).
[14] V. Kolevzon, J. Chem. Phys. (to be published).
[15] V. G. Levich, *Physicochemical Hydrodynamics* (Prentice Hall, New York, 1962).
[16] J. C. Earnshaw, R. C. McGivern, A. C. McLaughlin, and P. J. Winch, Langmuir **6**, 649 (1990).
[17] E. H. Lucassen-Reynders and J. Lucassen, Adv. Colloid. Interf. Sci. **2**, 347 (1969).
[18] H. Z. Cummins, in *Photon Correlation and Light Beating Spectroscopy* (Plenum, New York, 1974).
[19] J. C. Earnshaw and R. C. McGivern, J. Phys. D **20**, 82 (1987).
[20] D. Byrne and J. C. Earnshaw, J. Phys. D **12**, 1133 (1979).
[21] S. Hard, Y. Hamnerus, and O. Nilsson, J. Appl. Phys. **47**, 2433 (1976).
[22] M. Abramovich and I. A. Stegun, *Handbook of Mathematical Functions* (Dover, New York, 1972).
[23] A. C. McLaughlin and J. C. Earnshaw, J. Colloid Interf. Sci. **158**, 247 (1993).
[24] C. J. Hughes and J. C. Earnshaw, Phys. Rev. E **47**, 3485 (1993).
[25] L. D. Landau and E. M. Lifshitz, *Theory of Elasticity* (Pergamon, Oxford, 1986).
[26] V. Kolevzon (unpublished).